HST PHOTOMETRY AND SURFACE MAPPING OF ASTEROID 1 CERES. Jian-Yang Li, Lucy A. McFadden, *Dept. of Astronomy, University of Maryland, College Park MD 20742, (jyli@astro.umd.edu)*, Joel Wm. Parker, Eliot F. Young, *Dept. of Space Studies, SwRI, Boulder CO 80302*, Peter. C. Thomas, *Center for Radiophysics and Space Research, Cornell University, Ithaca NY 14853*, Christopher T. Russell, *IGPP & ESS, UCLA, Los Angeles CA 90095*, S. Alan Stern, *Dept. of Space Studies, SwRI, Boulder CO 80302*, Mark V. Sykes, *Planetary Science Institute, Tucson AZ 85719*.

Introduction: The first asteroid discovered in 1801, asteroid 1 Ceres, is among the oldest and most intact asteroids, and unique. The density of Ceres calculated from the most recent size measurement [1] indicates a large water fraction close to that of the solar system environment in early formation stages. However, because of the difficulty in interpreting its reflectance spectrum, and the lack of any spectral match with available meteorite samples [2,3], little is known about it. To resolve its surface, and to support NASA's Dawn Discovery mission, which will orbit Ceres starting in 2015 for eleven months [4], we observed Ceres with HST High Resolution Channel of the Advanced Camera for Surveys (HRC/ACS) for more than one rotation of Ceres.

Data reduction: The HST observations used here cover one full rotational period of Ceres at phase angle of 6.2°. Three filters centered at 555 nm, 330 nm, and 220 nm were used. The pixel scale at Ceres is about 30 km, corresponding to about 3.5° longitude/latitude at equator. To measure the reflectance in the standard unit, I/F, the brightness of Ceres is first calibrated to the standard magnitude at both heliocentric distance and range 1 AU. The apparent magnitude of the Sun at V-band, -26.75, is used to calculate the V-band reflectance, and a solar spectrum modulated by HST/ACS filter throughputs is used to determine the reflectance at the other two wavelengths.

Whole-disk photometry: The lightcurves of Ceres are plotted in Fig. 1. Both the shape and the amplitude of the lightcurves agree with earlier ground based observations at similar phase angles [e.g., 5,6,7]. The small lightcurve amplitude of only 0.04 magnitude is totally unexpected from Ceres' rotationally symmetric shape [1], and must be due to some non-randomly distributed albedo pattern on Ceres' surface.

The HST observations provide reflectance measurements at three wavelengths complementing earlier measurements for Ceres. Combining our observations with earlier ones [8,9], the spectrum of Ceres at UV-visible is plotted in Fig. 2, which is characterized by an absorption band centered at about 280 nm, with the width of about 100 nm, and about 30% of the reflectance at 555 nm. This absorption feature could be due to a charge transfer or a semi-conductor band, and is present in the spectra of many iron-bearing minerals and salts. However, it cannot be matched by any available laboratory measured UV spectra [10].

Disk-resolved analysis: With disk-resolved images of Ceres and the precisely determined but simple shape [1], the limb darkening characteristics of Ceres can be modeled. Taking other parameters that cannot be constrained from our HST images modeled from earlier ground-based observations (B_0=1.6, h=0.06, g=-0.40) [11], our modeling with Hapke's theory [12] resulted in good fit only for the central portion of Ceres' disk with i and $e < 50°$(V and U) or 40°(UV) with the residuals consistent with its lightcurve amplitude, and without any systematic deviation associated with i or e. The SSA at V-band is about 7%, yielding a geometric albedo of 9%, a value that is consistent with earlier results [5]. The roughness of Ceres is unusually high, and not consistent with the results measured from the ground [11], but consistent with what is inferred by IR observations [13]. Radar observations also indicate a surface that is very rough at scales larger than meters or tens of meters but very smooth at centimeter to decimeter scales [14]. Therefore, if the high roughness is real, the surface of Ceres must be made of very smooth materials, either like the surface of ice or deposited by very fine grained particles, but saturated with craters at the sizes of tens of meters to kilometers, even while it is globally relaxed.

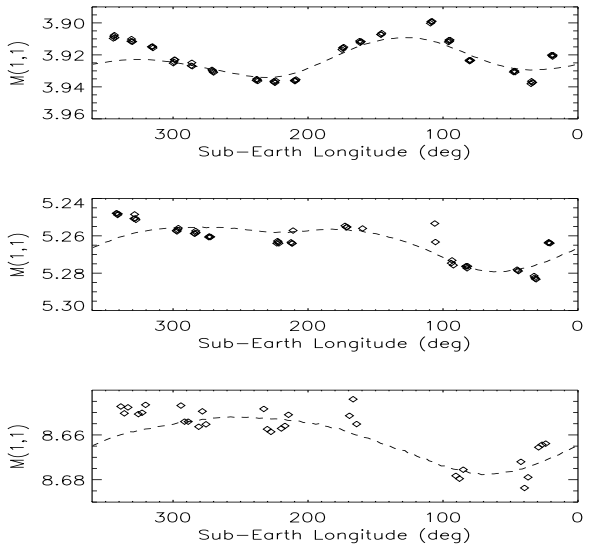

Figure 1: The lightcurves of Ceres are plotted as symbols for 555 nm (upper panel), 330 nm (middle panel) and 220 nm (lower panel). The synthetic lightcurves from our SSA maps are plotted as dashed lines.

A Minneart model was also used to model the limb darkening profile. Similar to Hapke's modeling, only the central portion of Ceres' disk can be fitted well with a Minneart model. Not consistent with earlier results [8], a smaller Minneart parameter of 0.6 was found, which is, however, consistent with the IR observations [13]. We think this is due to phase angle difference of earlier HST observations (19°), IR observations (9°), and our HST images (6.2°), thus indicating a stronger phase angle dependence of the Minneart parameter for Ceres' surface than that for the icy satellites of Uranus [15].

Albedo Map: Since the total reflectance of dark surfaces like

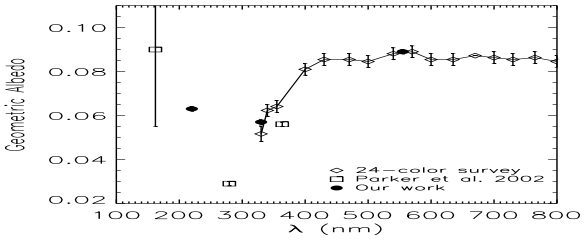

Figure 2: The spectrum of Ceres constructed from our measurement and earlier work.

Ceres is proportional to SSA, the ratio of HST images and their corresponding model from disk-averaged limb darkening models yields the SSA map of Ceres' surface. By combining all HST images covering the whole surface of Ceres, we constructed global SSA maps (Fig. 3) for low latitude area on Ceres that can be photometrically modeled. Three tests confirmed that a few percent SSA variations over Ceres' surface are real. First, the superior SNR of higher than 1000 for our HST images, as well as our error estimate, indicates the relative photometric error of 2% for the UV-band map, and smaller for the other two wavelengths. Second, we inspected animations of Ceres' rotation both before the images are projected onto a longitude-latitude plane and after. Those two animations confirmed that, first, we do see features in the raw HST images; and second, every feature in different images are projected correctly, and positively enhanced to show themselves in final maps. And third, we used our SSA map to produce synthetic lightcurves as plotted in Fig. 1 by dashed curves. Their similar shapes indicate a correct mapping of the overall brightness distribution. The largest discrepancy appears at longitude about 0° at all three wavelengths with about 1.4% underestimate by the model, compared to the 4% total lightcurve variation.

The distribution of the SSA of Ceres at three wavelengths all show a unimodal shape with very narrow ranges ($\leq$3%). The upper limit of color variation determined from the SSA variations should not exceed 5%. The SSA and color variations of Ceres are much smaller than those of other asteroids that contain no water, but very similar to those of the icy moons of giant planets. Ceres has the most uniform surface of solar system small bodies measured to date. This is probably related to the possible resurfacing process involving water, and consistent with the most recent evolution model of Ceres [16].

Albedo Features: All features are almost consistent at three wavelengths (Fig. 3). The most obvious one is the big bright area (2) centered at 130° longitude and 15° latitude, about 50° across, with an elongated shape. Other features are almost all circular, including the one at 0° longitude (1). A series of circular features (3-5) exist along the diagonal line to the right of the largest bright area. A dark area (7) to the left of the largest bright area is open toward the south pole. Another dark area (8) that has a bright rim enclosed to the right of the largest bright area is consistently dark at all three wavelengths, and it is most likely to be the "Piazzi" feature observed and named from earlier HST observation [8].

Comparing the SSA maps at three wavelengths, we can notice that the features can be divided into at least two different color groups. One is represented by spot 2, which is about by 8% relatively redder than the second group that includes no. 1 and 3-5. This difference is also confirmed by the different shapes of lightcurves at three wavelengths. The spectral variation between those two groups of features, and their different shapes, may indicate different compositions and origins.

References: [1] P. C. Thomas *et al.*, in preparation; [2] C. R. Chapman & J. W. Salisbury (1973), *Icarus* **19**, 507; [3] T. V. Johnson & F. P. Fanale (1973), *J. Geophys. Res.* **78**, 8507; [4] C. R. Russell *et al.* (2004), *Planet. Space Sci.* **52**, 465; [5] E. F. Tedesco *et al.* (1983), *Icarus* **54**, 23; [6] R. D. Taylor *et al.* (1976), *Astrophys. J.* **81**, 778; [7] H. J. Schober (1976),*Mitteilungen der Astronomischen Gesellschaft* **40**, 207; [8] J. W. Parker *et al.* (2002), *Astron. J.* **123**, 549; [9] C. R. Chapman & M. J. Gaffey (1979), in *Asteroids*, 655; [10] J. K. Wagner *et al.* (1987), *Icarus* **69**, 14; [11] P. Helfenstein & J. Veverka (1989), in *Asteroids II*, 557; [12] B. Hapke (1983) *Theory of Reflectance and Emittance Spectroscopy*, Cambridge University Press; [13] O. Saint-Pe *et al.* (1993), *Icarus* **105**, 271; [14] D. L. Mitchell *et al.* (1996), *Icarus* **124**, 113; [15] J. Veverka *et al.* (1989), *Icarus* **78**, 14; [16] T. B. McCord & C. Sotin (2005), *J. Geophys. Res.*, in press

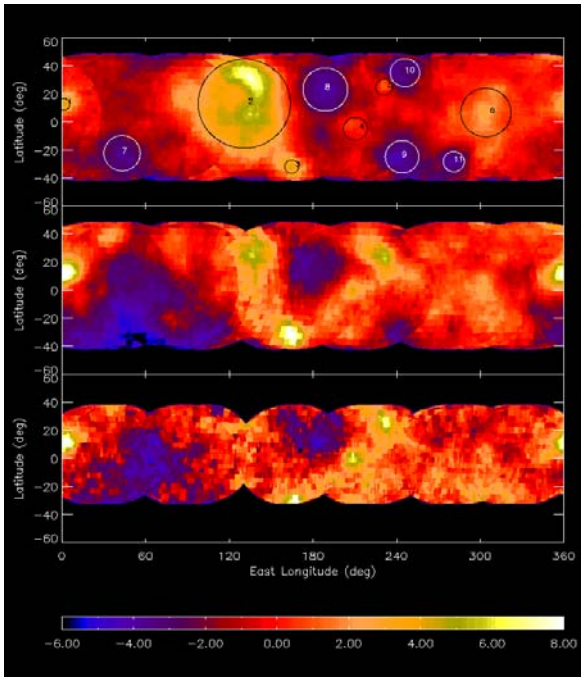

Figure 3: The SSA maps at 555 nm (upper panel), 330 nm (middle panel), and 220 nm (lower panel). The color bar represents the percentage deviation of the SSA from averages, which are 0.070, 0.045, and 0.050 at three bands, respectively. The circles with numbers in the upper panel mark the features we identified. From 1 to 6 are bright features, and from 7-11 are dark features.